Proceedings of the 3rd International Conference on the Frontiers of Plasma Physics and Technology (PC/5099)

Relativistic Electron Heating in Focused Multimode Laser Fields with Stochastic Phase Purturbations

Yu.A.Mikhailov, L.A.Nikitina, G.V.Sklizkov, A.N.Starodub, M.A.Zhurovich
P.N.Lebedev Physical Institute, Leninsky pr 53, Moscow

Abstract

A direct relativistic electrons acceleration simulation model with a given electromagnetic field which is determined by wave packet parameters is considered. The multimode time-spatial structure of focused Nd-laser beam with stochastic phase disturbances of each spectral component is taken into account as a source of random forces. The electron energies more than 10 MeV are derived even at moderate flux densities of 10^{16} W/cm^2. The developed numerical code gives it possible to obtain quantitative energy distribution function in relation to both field intensities and temporal U-shape of laser pulse. The efficient heating of electrons can be triggered in the presence of counter propagating wave being reflected from critical plasma area with varied reflection coefficient. The heating mechanism occurs with a delay relative to the beginning of the pulse when the laser fields exceed some threshold amplitudes. The qualitative comparison of simulation results with the experimental data is given as evidence that this mechanism is not unreasonable.

1 Introduction

Generation in a laser plasma electrons with an energy many times greater than that of the thermalized electrons is an extremely important physical phenomenon. Study of the generation and acceleration of fast electrons in a laser plasma makes it possible to understand and investigate some complicated physical processes that can accelerate electrons to very high energies. Examples of such processes are the resonant absorption of laser radiation in a plasma and parametric instabilities near the critical density, two-plasmon decay in the region of the quarter-critical density, stimulated Raman scattering in plasma coronas and discussed in this report relativistic electron heating in focused multimode laser fields with stochastic phase perturbations. From the practical point of view, it is very promising to use a laser plasma that generates fast electrons as the cathode of an injector of high-current pulsed accelerators since such laser-plasma cathodes can, compared with traditional types of cathodes, ensure a high initial energy of the electrons (>10^2 keV), a short duration of the injection pulse (<10^{-9} s), and huge current densities (>10^6 A/cm^2). The generation of fast electrons in a laser plasma can play a very important role for the purposes of laser thermonuclear fusion. In schemes of hydrodynamic acceleration and compression of thermonuclear targets, even a small number of high-energy electrons, carrying less than 1% of the absorbed laser energy penetrating into the central region of the target can, cause it to be preheated and thereby catastrophically lower the compression by more than an order of magnitude and prevent the attainment of the necessary value of the confinement parameter ρR (ρ, R – are the density and radius core of a target). On the other hand, in the currently widely discussed promising scheme of laser thermonuclear fusion known as "fast ignition" one of the decisive factors in achieving success is the possibility of generating in the coronal region of the thermonuclear target high-energy electrons under the influence of an ultrashort pulse of laser radiation in order to ensure effective transport of energy via these electrons into the ignition region. In many experimental works the superthermal electrons have been observed. The presence of hot electrons resulted in appearance of high energetic ions and anomously hard X-ray emission spectrum. The most recent papers dealt with hot

electron observation are concerned with laser plasma produced by femptosecond laser radiation focused onto solid target at flux densities of $10^{18}-10^{20}\,W/cm^2$. The relativistic factor is much more than unity at such radiation densities. There are a few experiments in the range of $10^{13}-10^{15}\,W/cm^2$ and at nanosecond pulse duration in which anomously energetic electrons (essentially more than oscillatory energy) were registered. The most important is the fact that the significantly large part of incident laser energy was converted into energy of hot electrons. In a number of works the different stochastic acceleration mechanisms were considered to explain anomalous energy of electrons when spontaneous self generated magnetic fields or plasma wave beating or wake fields were used as a source of random perturbation of momentum of an electron. See for example [1-4]. Laser energy transfer and enhancement of plasma waves and electron beams by interfering high-intensity laser pulses were considered in [5].

In the present paper, we consider a mechanism of stochastic electron heating under critical homogeneous electron density and at focal intensities in the range of $10^{13}-10^{17}\,W/cm^2$ which are important for direct fusion target heating. The field random phase distribution over focal plane (speckle structure of intensity) as well as phase beating in wave packet of multimode Nd-laser beam of 3ps duration are taken into account as a source of random forces in equation of motion of charged particle. The dependence of electron energy distribution function shape and dependence of mean energy on focal intensity was obtained numerically. The calculation of trajectories of 2000 electrons resulted in their directivity at output equaled to $\sim 0.7\,rad$. The reflected from critical area wave was taken into account.

2 Intensity and field distribution in the focal plane

The focal intensity distribution was measured for aspherical lens with focus 10cm and aperture of the beam 45mm. Then we reconstruct field distribution numerically by choicing the structure of beam which corresponded to the focal intensity. We use an angle structure consisting of several tens of angular modes, so the total divergency was about $\sim 2\cdot 10^{-4}\,rad$. In Figs. 1 and 2 typical intensity and field distributions are given for focal Y-Z plane.

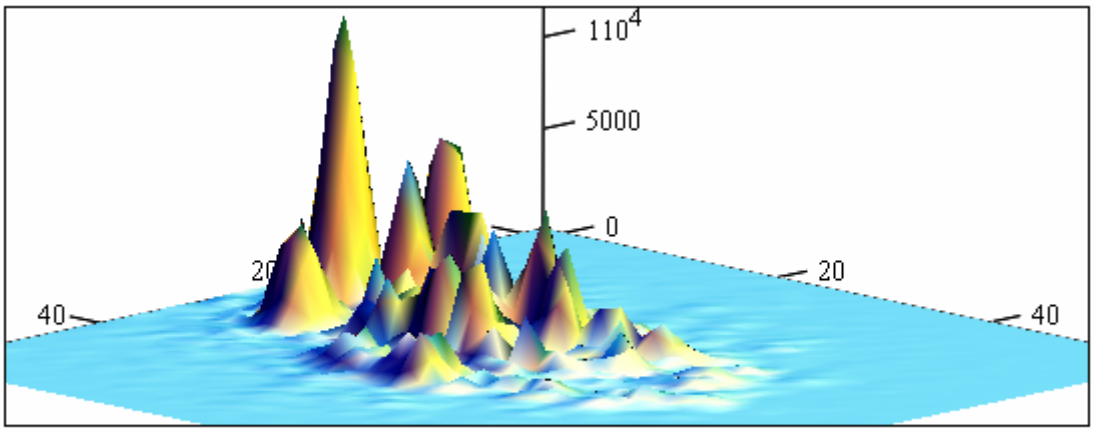

Fig.1. Typical focal intensity distribution.

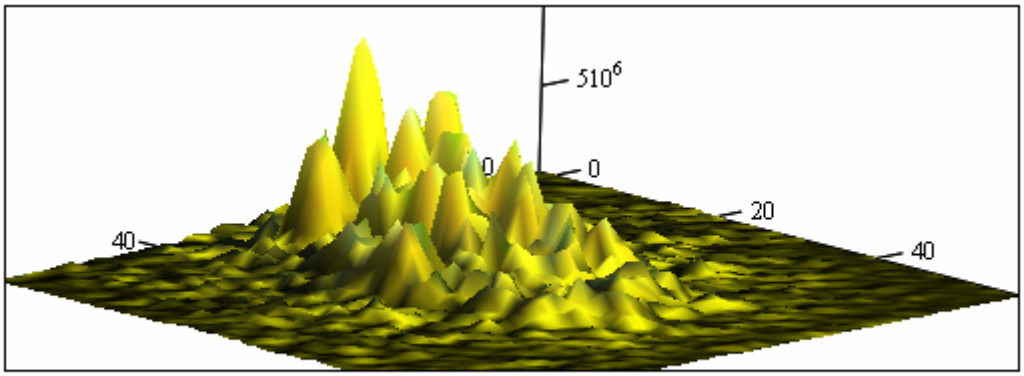

Fig.2. Typical field intensity distribution.

Polarized E-field phase distribution is shown on the Figs. 3 and 4.

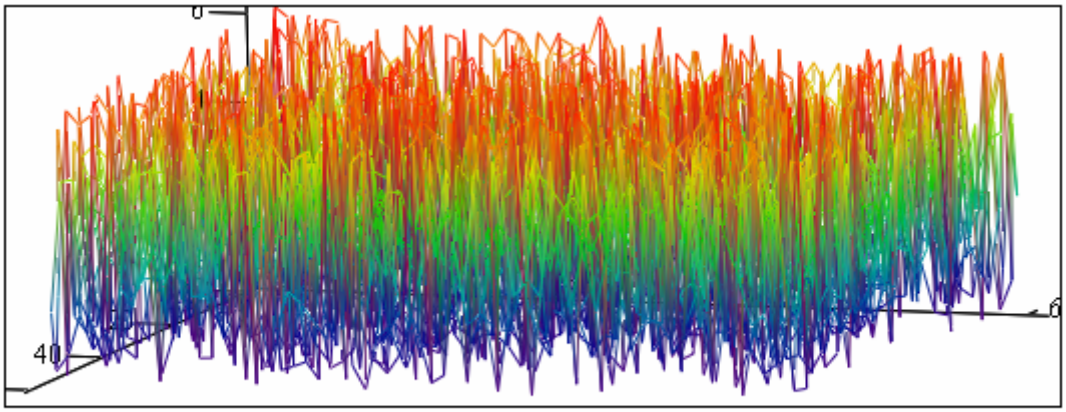

Fig.3. Electric field phase distribution over the focal Y-Z plane.

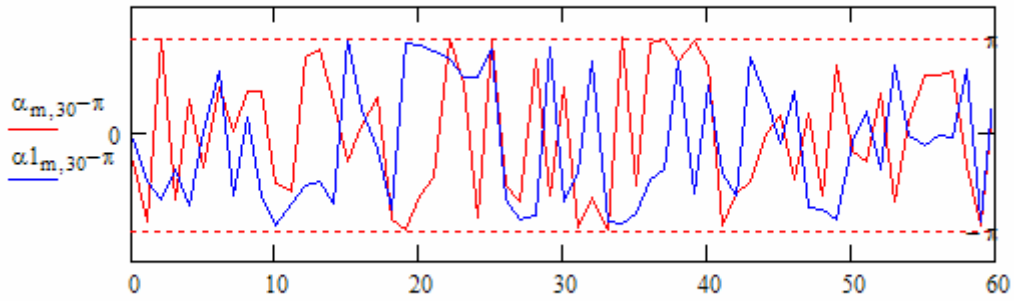

Fig.4. Field phase over focal plane.

Here are the field phase traces for two perpendicular crossections, $y = 0$, or $z = 0$. Note that the phase changes randomly over Y-Z plane from π to minus π. The relative phase shift between two successive maximum or minimum of R-field is shown. The absolute phase shift therewith is defined with the accuracy $2\pi n$, where $n-$ is integer.

3 The model

The model describes the acceleration of charged test particles in a given electromagnetic field formed in focal area by polarized incident and reflected light beams. The incident and reflected beams consist of a few frequency components each. The complicated phase structure of focal intensity speckle patterns was approximated by regular phase perturbation in time with random phase shock amplitude. The frequency of phase shocks which electron meets along its motion trajectory corresponds to 2/3 of critical plasma frequency. A moving electron experiences a electromagnetic field the phase of which changes sharply in a time rather less than wavelength period. Then the phase is constant until the next phase jump occurs. The random spread of relative phase of each spectral component was taken into account. The temporal shape of laser beam wave packet was U-shape which approximate by envelope function $\delta(t)=\left[\left(1-\frac{t}{\tau}\right)\cdot\frac{t}{\tau}\right]$. The multi component spectral line of laser radiation approximated by the function $f(j)=\left(1-\frac{j}{N_L}\right)\cdot\frac{j}{N_L}$ where $j-$ is component number, N_L- the number of components. For example Nd-glass radiation usually consists of twelve spectral components. However in this work we consider only four components to simplify and quicken numerical procedure. The phase factor of a component is represented by expression $f_e(j,t)=\exp\left(i\cdot\left[\omega_0\left[1+\left(\frac{\Delta n_\lambda}{n_\lambda}\right)\cdot\left(j-\frac{N_L}{2}\right)\right]\cdot\left(t-\frac{\tau}{2}\right)-\Phi_j\right]\right)\cdot f(j)$, where ω_0- frequency at the maximum of spectral line, $n_\lambda-$ number of periods in pulse duration τ, $\Delta n_\lambda-$ frequency interval in number of periods between neighboring equidistant spectral components, Φ_j- random phase but not more than it follows from uncertainty condition. For example in the case of polarized field we can write $E_y(\vec{r},t)=A(y,z)\cdot\left(\sum_{j=0}^{N_L}f_e(j,t)\right)\cdot\left[(1-\gamma)\cdot e^{-ik_x x}+2\gamma\cos k_x x\right]\cdot\delta(t)\cdot e^{i\psi(t)}$, and $H_z(\vec{r},t)=A(y,z)\cdot\left(\sum_{j=0}^{N_L}f_e(j,t)\right)\cdot\left[(1-\gamma)\cdot e^{-ik_x x}-2i\gamma\sin k_x x\right]\cdot\delta(t)\cdot e^{i\psi(t)}$, where $k_x\approx\frac{2\pi}{\lambda}$ - wave number, $\psi(t)-$ random function, $\gamma=\frac{E_{refl}}{E_{inc}}$ - amplitude reflection coefficient. The longitudinal and depolarization parts of fields are written by the similar way. They does not influence essentially on the electron stochastic motion at least on the level of 20% of field amplitude. In our model spatial nonuniformity of a field does not influent a great deal on energy gain in contrast to work [6].

4 Stochastic Equations of Motion

To investigate the acceleration of test particles in the electromagnetic fields formed as described above, we consider the relativistic equations of motions of a positive electron in a given external electromagnetic field: $\frac{d\bar{r}'}{dt'}=v'(\bar{p}')$; $\frac{d\bar{p}'}{dt'}=\frac{q}{c}\cdot\bar{v}'(\bar{p}')\times\bar{B}(\bar{r}',t')+q\cdot\bar{E}'$. Here are unknown variables: p_x', p_y', p_z', x, y, z, here the dotted values related to real values. For the numerical integration, we express equations in terms of the following

relations: $t = ct'$, $\vec{p} = \frac{\vec{p}'c}{mc^2}$, $T_{kin} = \frac{T'_{kin}}{mc^2}$, $\vec{V} = \frac{\vec{V}'}{c}$, $E = \frac{qE'}{mc^2}$, $B = \frac{qB'}{mc^2}$. Now we write the reduced equations in the form:

$$\begin{cases} \frac{d\vec{r}}{dt} = \vec{\beta}(\vec{p}), \quad \vec{\beta}(\vec{p}) = \frac{\vec{p}}{\sqrt{1+(\vec{p}\cdot\vec{p})}}, \\ \frac{d\vec{p}}{dt} = \vec{\beta}(\vec{p}) \times \vec{B}(\vec{r},t) + \vec{E}(\vec{r},t). \end{cases}$$

Here time t expressed in cm. Coordinates x, y, z are unchangeable that are in cm. The reduced energy T and momentum p_x, p_y, p_z assigned in units of electron rest energy mc^2. The particle motion equations are solved with a 4th order Runge-Kutta adaptive step-size scheme. In numerical calculations we analyze the motion of 1000-2000 free electrons. The laser pulse duration is ~3.5ps which is appropriate to 1000 wavelengths. The pulse shape was approximated by parabola function $\delta(t)$ with high contrast ratio which is rather differ from Gauss shape. The electrons gain the most part of energy only in the X-Y plane in spite of 3D trajectory. We consider the uniform neutral cloud of nonintaracting electrons in spatially and time modulated electromagnetic fields. The test electrons start acceleration within the simulation box at random positions. Momentum initial conditions corresponded to normal distribution with temperature of ~0.5keV, which represents a typical value in laser plasma corona near critical area for focal intensities under consideration in present work. The simulations were performed with a resolution of 50 cells per laser wavelength and time step was carefully chosen to ensure that numerical dispersion was not a factor.

5 The Electron Trajectories

In Fig.5 a set of trajectories projected on to X-Y plane of typical test electrons is shown. The end of a trajectory is consistent with the end of the wave packet subsequent to electromagnetic fields are switched off. It can be seen that during irregular motion a particle is subjected to a random force than stronger than its momentum is lower. When a stochastic acceleration is developed the motion of particles becomes directional. The most part of electrons moves in the direction of incident wave propagation. It is notable that about half of particles moves inside the angle of ~0.7 rad (in the case of 2000 particle trajectories analysis). In the case of long pulses of 3.5ps and 10ps duration the directivity of particle motion does not depend on initial phase position that is on the random initial position in simulation box. The same regards to random initial energy of a particle. This fact confirms the stochastic nature of motion under electromagnetic field phase perturbation. In this case electric field E_y and magnetic field B_z were polarized. The longitudinal components of electromagnetic fields has not taken into account. The small depolarization ~5% does not influence on the trajectories a great deal. Each incident field consists of two frequency components with frequency interval $\Delta\omega = \omega_0/500$ and with random relative phase. The reflection coefficient was equal to $\gamma = 0.2$. When reflection is close to unity $\gamma > 0.8$ The electron motion reminds one of the case of standing wave. The directivity of electron motion to the end of the pulse therewith becomes almost isotropic.

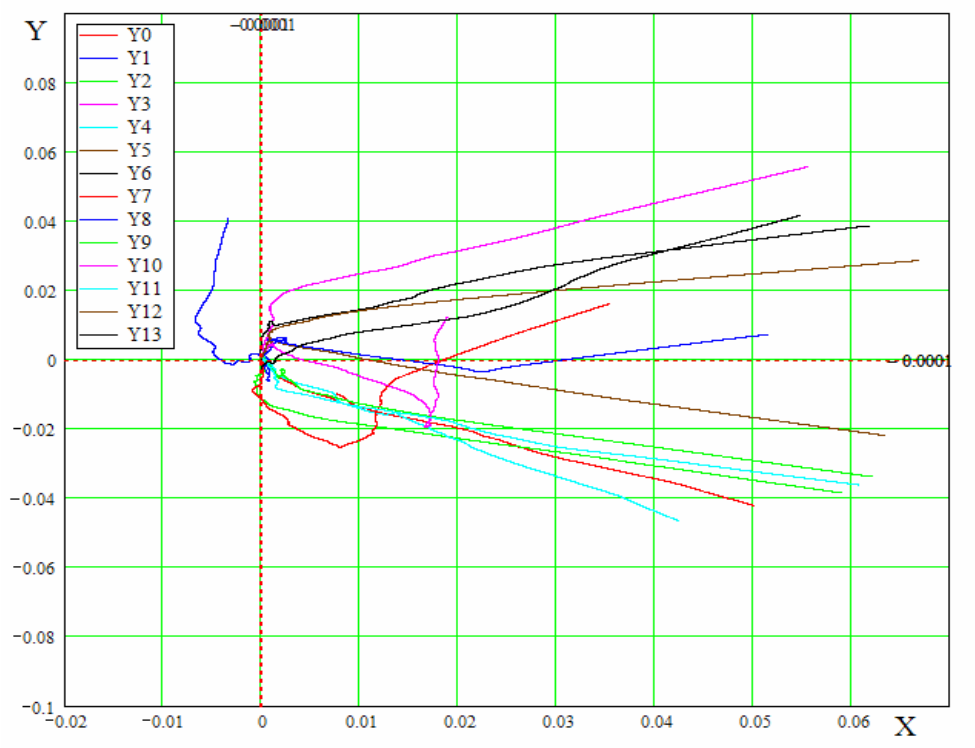

Fig.5. Trajectories projected on to X-Y plane for typical test electrons. X [cm] is parallel to wave vector $\vec{k}$; Y [cm] parallel to E. The fourteen curves are taken by an arbitrary way.

In the Fig.6 the early stage of particle acceleration is shown. It is easy to see that the initial stage of motion of a particle strongly dependent on random initial energy and space phase position in simulation box. However at the early times that is a few tens of wave periods the increase of stochastic energy of a particle is not noticeable. The direction of initial particle moving is dependent on random initial phase and the values of momentum components. In some cases a long linear part of trajectory can be seen that implies to the minimum of magnetic field in the point of initial position of a test particle.

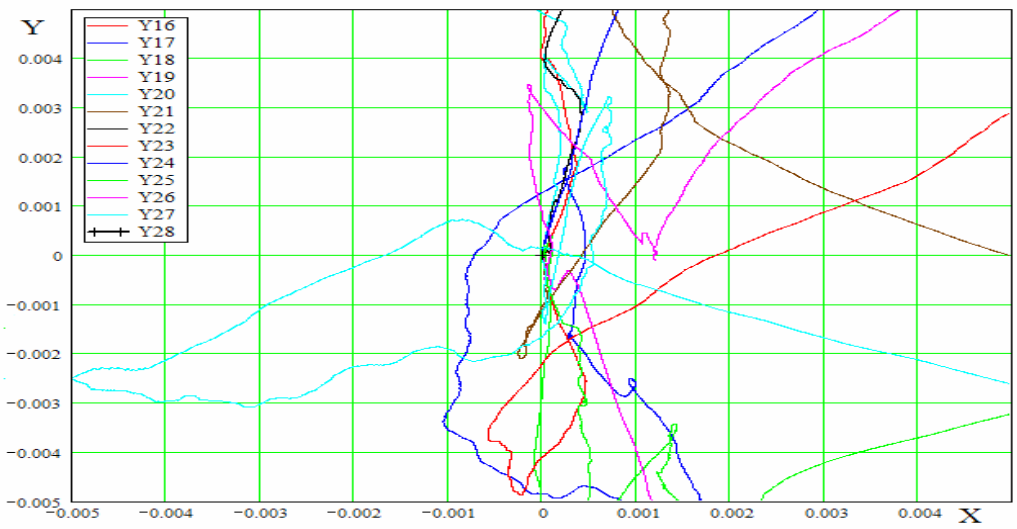

Fig.6. The early stage of particle trajectories X [cm] is parallel to K; Y [cm] parallel to E.

6 The energy gain of a particle during laser pulse

In Fig.7 the time evolution of the kinetic energy of a test electron for fixed field intensity corresponded to light intensity $q = 2 \cdot 10^{17}\, W/cm^2$ is shown. There are typical fifteen randomly selected traces from 1000 ones. Initial conditions are as mentioned above. The time [in cm] is plotted on X-axis. A vertical division is equaled to 10MeV for each trace. The field is switched off at 0.1cm for convenience of observation. It is easily seen that stochastic process of a particle acceleration develops after some delay which varies from tens to hundreds of wavelengths. This delay is longer than for the case of rectangular pulse when the field switched on instantaneously. The damping of small variations is related to the decrease of field intensity on the slope of the pulse. The small structure of an energy evolution trace account for force perturbations which resulted in the direction change of momentum of a test particle.

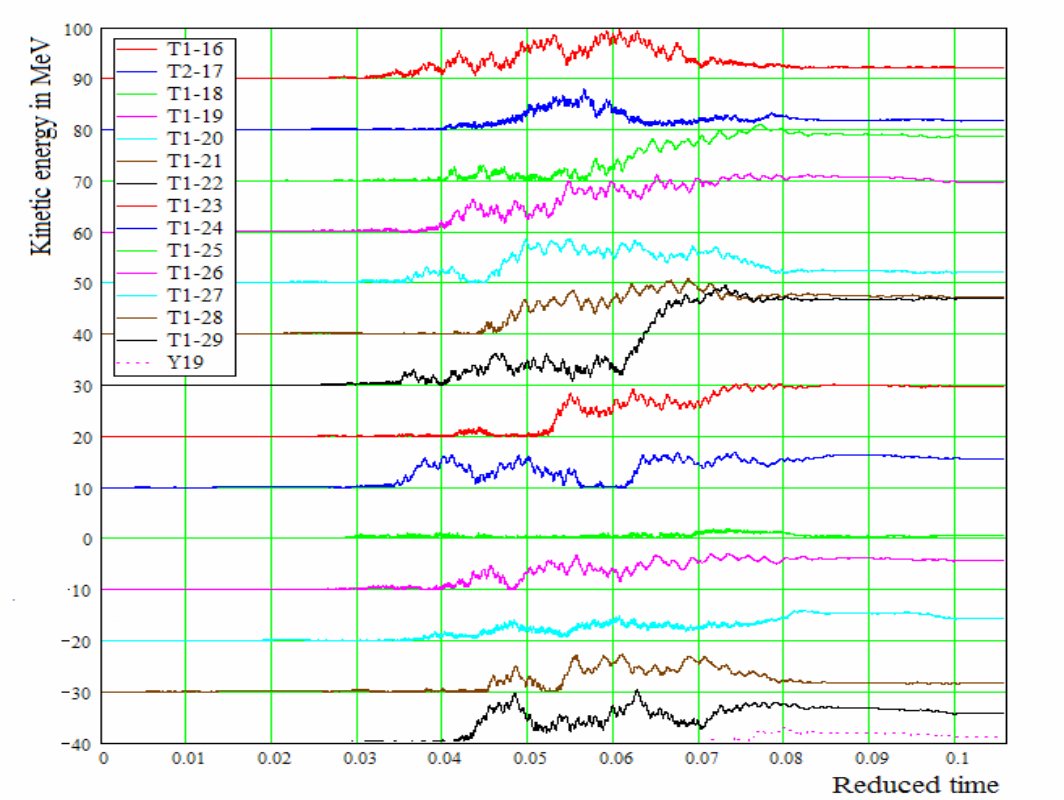

Fig.7. The time evolution of the kinetic energy of a test electron for fixed field intensity corresponded to light intensity $q = 2 \cdot 10^{17}\, W/cm^2$. Each cell in vertical axis is equal to 10 MeV for corresponding curve. Pulse duration is 3.5 ps.

7 Energy Spectrum of Electrons

In the Fig.8 the distribution functions of electrons normalized to the maximum probability for different field intensities are presented. The figure denoted by "mean" implies to the energy averaged over a proper curve. The figure denoted by "max" implies to the

energy related to maximum energy of all electrons the energy of each averaged over the time of field action. The parameter eb implies the value of field intensity in terms of Mega $CGSE/cm$. For example $eb = 20$ is matched to power density of $q = 10^{17}\, W/cm^2$. The parameter $eb = 0.5, 1, 2, 3, 4, 5, 10, 20$ in Fig.8 denote distribution functions corresponding to field intensities equaled to $6\cdot10^{13}$, $2.5\cdot10^{14}$, 10^{15}, $2\cdot10^{15}$, $4\cdot10^{15}$, $5.2\cdot10^{15}$, , $2.5\cdot10^{16}$, 10^{17} W/cm^2. The energy distribution functions are not Maxwellian, they have a long energetic tail.

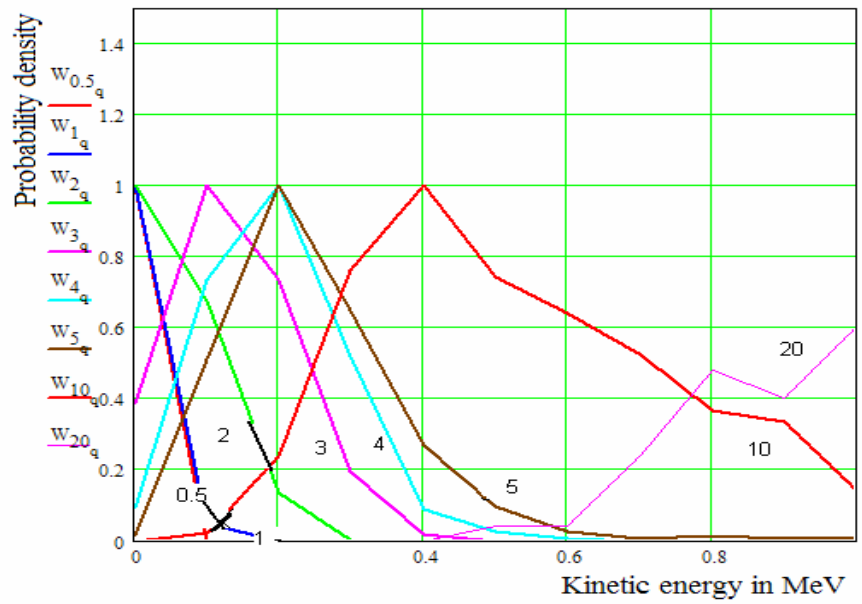

Fig.8. The distribution functions of electrons normalized to the maximum probability for different field intensities. Numerals near the curves denote distribution functions corresponding to field intensity parameter eb.

In the Fig.9 the curves denoted by "output energy probability" correspond to energy distribution functions of electrons at the end of the laser pulse ~3.5ps. The curves "cutoff energy probability" shows the fractional number of electrons having the energy more than corresponding figure on X-axis. The curves "cutoff current" show the normalized current which can be registered by a detector outside interaction area. It can be seen from these graphs that at flux density $10^{17}\, W/cm^2$ more than 20% of electrons can have energies more than 6 MeV. Here "output energy probability" means energy distribution of 1000 electrons at time equaled to 90% of pulse duration. The "cutoff energy probability" means the fraction of particles having energy which exceeds the corresponding value on X-axis. The "cutoff current" means the fractional current value of electrons which escape focal area and have the energy more than the value on X-axis one. The parameter eb indicates the value of field intensity in units of $10^6\, CGSE = 3\cdot10^8\, V/cm$. The dotted curves designated by "cutoff current" show the probability of total flow of particles which escape the interaction area. It is really electric current which can be measured like it was done in previous work at intensities $10^{13} \div 10^{15}\, W/cm^2$.

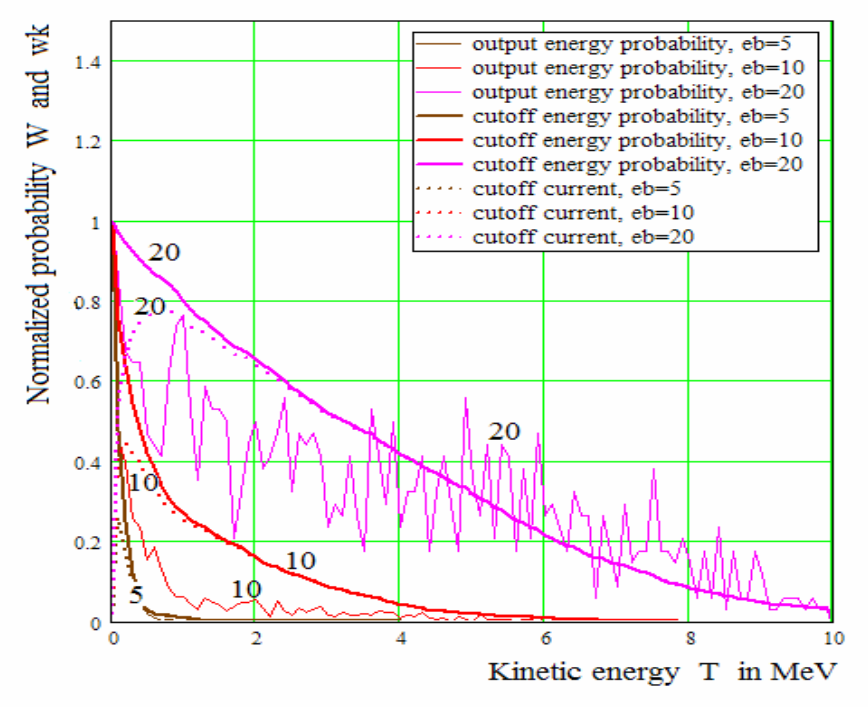

Fig.9. Energy distribution functions of electrons at the end of the laser pulse ~3.53ps.

The curves "cutoff energy probability" show the fractional number of particles which have energy more than the energy on X-axis. At flux density $q = 10^{17}\, W/cm^2$ $(eb = 20)$ the energy distribution function is not smooth that is not simply explainable. We can say only that this is not associated with numerical procedure at least in the framework of approximation model given above. The data given in the Fig.9 result in large amount of electrons which have energy rather more than relativistic oscillatory energy. For example the fractional part of electrons which have energies more than 350 keV is equal to ~15% even at relatively low intensity $\sim 6\cdot 10^{15}\, W/cm^2$, and the same 15% part of electrons have energies more than 2 MeV at intensity $\sim 2\cdot 10^{16}\, W/cm^2$. These curves were obtained by processing of 2000 electrons trajectories which were calculated with 80 cells per wavelength $(\lambda = 1.06\,\mu m)$.

8 The discussion

In the Fig.10 we attempt to compare the simulation results with experimental data. The points were obtained by measuring total cutoff electron current from copper solid target. The cutoff current is expressed by $j_{cutoff} \sim \int_T^\infty w(T)\cdot \frac{\sqrt{T(T+2)}}{T+1}\, dT$, where $w(T)$ - electron energy distribution function. Here the red two diamonds correspond to intensity $\sim 10^{16}\, W/cm^2$ which measure as averaged over focal spot and in time. Indeed there are spikes of intensity a few times more than averaged intensity. So these points can be compared with the red curve calculated at intensity $2.5\cdot 10^{16}\, W/cm^2$. The three brown

diamonds were measured at focal intensity $\sim 10^{14\div 15}\, W/cm^2$. We try to comply these points with the brown curve which calculated at intensity $6\cdot 10^{15}\, W/cm^2$. The bold curve for the current was calculated at intensity $10^{17}\, W/cm^2$ $(eb = 20)$. It illustrates that half of electrons gain energy more than 3 MeV. Qualitatively it is not contradictory to results obtained experimentally with femptosecond pulses. But quantitative comparison is not possible. Nevertheless the model in which random phase perturbation of focal field phase is taken into account can be considered a real possibility to explain the appearance of anomously energetic electrons in laser plasma at moderate intensity density. It is notable that up to 30% of absorbed laser energy was converted in electrons with mean energy exceeding 600keV at 0.5ps, 15J, $\sim 10^{19}\, W/cm^2$ [2], and up to 30% of absorbed laser energy was the energy of target charge due to 300 keV electrons at 2 ns, $\sim 10^{14}\, W/cm^2$ and 3.53ps, $\sim 10^{15}\, W/cm^2$ pulses [1].

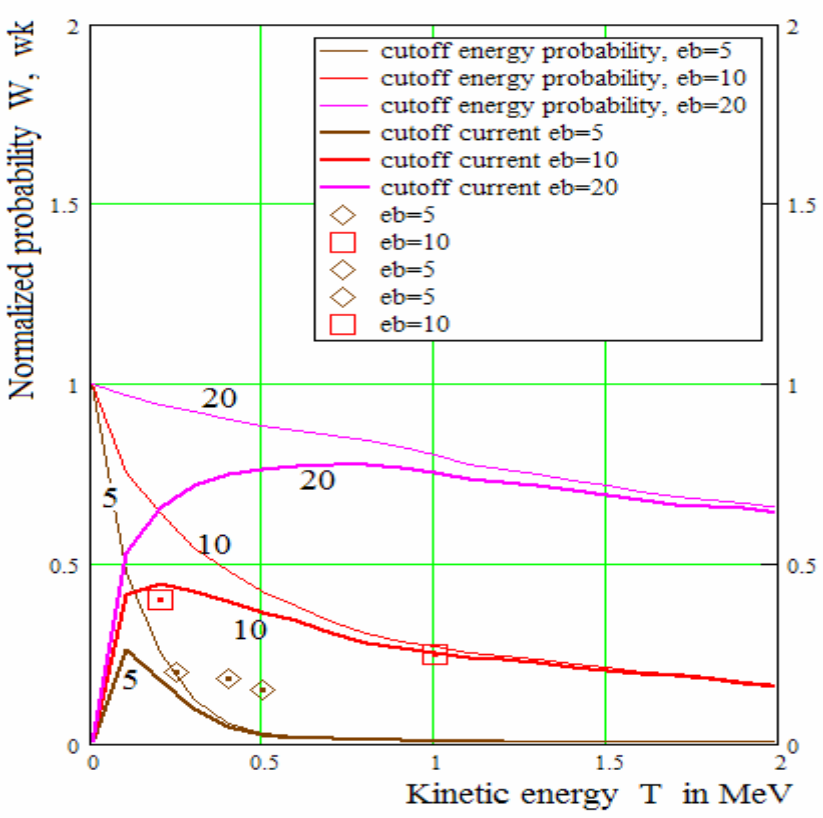

Fig.10. Comparison of the simulation results with experimental data.

The processing of data obtained by simulation resulted in dependence of electron energies on focal laser power density which is consistent with our theoretical model. The four curves are shown in the Fig.11 where in X-axis the intensity and in Y-axis energy are plotted in absolute units. The upper curve (diamonds) shows the dependence of maximal energy on intensity. The next lower curve (circles) shows the dependence of maximal energy during pulse averaged over 1000 electrons on intensity. The next lower curve (boxes) related to averaged energy of the electrons at the end of the pulse. Finally the lowest curve (crosses)

related to electron energy averaged over all electrons and averaged over the pulse for each electron.

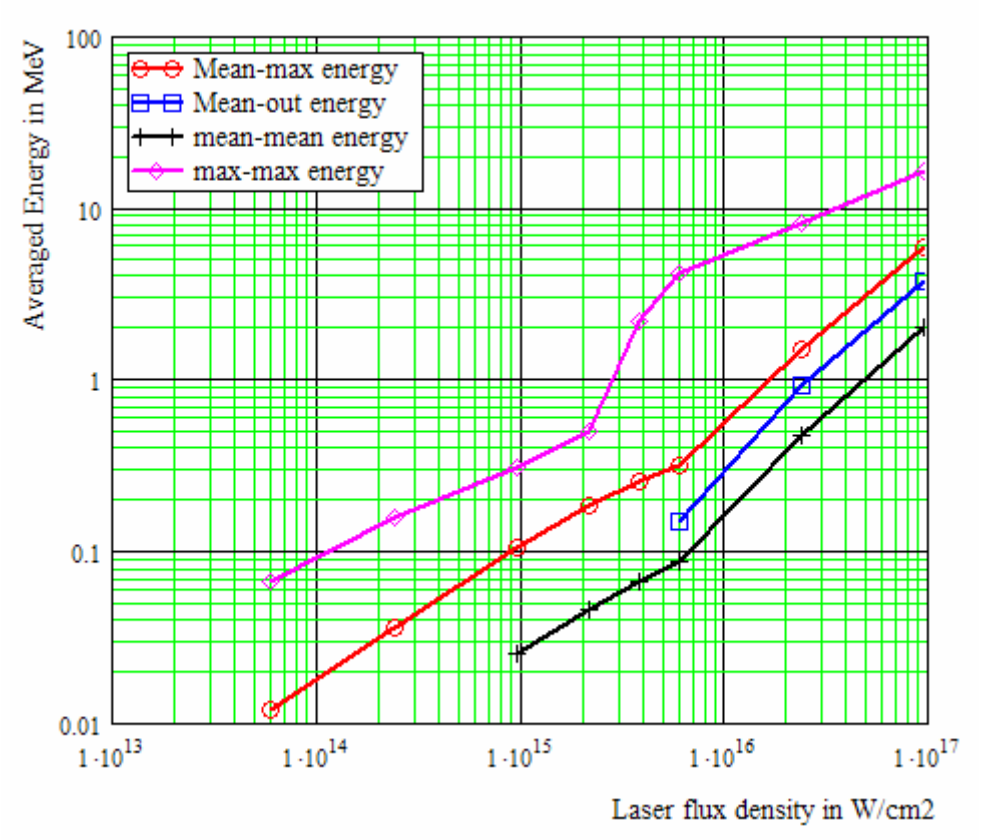

Fig.11. The dependence of maximal energy on intensity (diamonds). The dependence of maximal energy during pulse averaged over 2000 electrons on intensity (circles). The averaged energy of the electrons at the end of the pulse (boxes). The electron energy averaged over all electrons and averaged over the pulse for each electron (crosses).

It is reasonable to consider the last dependence as some effective characteristic "temperature" T_{eff} of hot electrons under stochastic acceleration. In the range of intensities $6\cdot10^{13}\div6\cdot10^{15}\,W/cm^2$ the dependence looks like $T_{eff}\sim q^{0.45\div0.55}$ at wavelength $\lambda=1.06\,\mu m$. In the range of intensities $6\cdot10^{15}\div10^{17}\,W/cm^2$ the power increases $T_{eff}\sim q^{0.8\div0.9}$. Thus than intensity density approaches to relativistic one than the power of this dependence becomes more close to unity.

Acknowledgements

Authors would like to thank V.V.Klimov and V.V.Okorokov for useful discussions.

References

[1] V.V.IVANOV, et al., "Investigation of the generation of high-energy electrons in a laser plasma", JETP 82 (4), (1996), pp. 677-682.
V.V.IVANOV, et al., "Method of fast electron observation in laser plasma", Prib. Tekn, Eksp. 4, (1995), p.77.

[2] M.H.KEY, et al., "The potential of fast ignition and related experiments with a petawatt laser facility", Journal of Fusion Energy, 17 (1998), pp.231-236.

[3] ZHENG-MING Sheng, et al., "Efficient acceleration of electrons with counterpropagating intense laser pulses in vacuum and underdense plasma", Phys. Rev. E 69, (2004) 016407.

[4] Y.SENTOKU, et al., "High-energy ion generation in interaction of short laser pulse with high-density plasma", Appl. Phys. B 74 (2002), pp. 207-215.

[5] P.ZHANG, et al., "Laser energy transfer and enhancement of plasma waves and electron beams by interfering high-intensity laser pulses", PRL 91 (2003) 225001-1.

[6] E.V.Maiorov, et al., “Acceleration by nonuniform stochastic fields”, Preprint 9-04 (2004) Inst. Theor. Exp. Phys., Moscow.